A&A 540, L9 (2012)
DOI: 10.1051/0004-6361/201219042

Astronomy & Astrophysics

Letter to the Editor

An upper limit to the variation in the fundamental constants at redshift $z = 5.2$

S. A. Levshakov[1,2], F. Combes[3], F. Boone[4], I. I. Agafonova[1,2], D. Reimers[1], and M. G. Kozlov[1,5,6]

[1] Hamburger Sternwarte, Universität Hamburg, Gojenbergsweg 112, 21029 Hamburg, Germany
[2] Ioffe Physical-Technical Institute, Polytekhnicheskaya Str. 26, 194021 St. Petersburg, Russia
e-mail: lev@astro.ioffe.rssi.ru
[3] Observatoire de Paris, LERMA, CNRS, 61 Av. de l'Observatoire, 75014 Paris, France
[4] Université de Toulouse, UPS-OMP, CNRS, IRAP, 9 Av. colonel Roche, BP 44346, 31028 Toulouse Cedex 4, France
[5] Petersburg Nuclear Physics Institute, 188300 Gatchina, Russia
[6] St. Petersburg Electrotechnical University "LETI", Prof. Popov Str. 5, 197376 St. Petersburg, Russia

Received 15 February 2012 / Accepted 15 March 2012

ABSTRACT

Aims. We constrain a hypothetical variation in the fundamental physical constants over the course of cosmic time.
Methods. We use unique observations of the CO(7–6) rotational line and the [C I] $^3P_2 - ^3P_1$ fine-structure line towards a lensed galaxy at redshift $z = 5.2$ to constrain temporal variations in the constant $F = \alpha^2/\mu$, where μ is the electron-to-proton mass ratio and α is the fine-structure constant. The relative change in F between $z = 0$ and $z = 5.2$, $\Delta F/F = (F_{\rm obs} - F_{\rm lab})/F_{\rm lab}$, is estimated from the radial velocity offset, $\Delta V = V_{\rm rot} - V_{\rm fs}$, between the rotational transitions in carbon monoxide and the fine-structure transition in atomic carbon.
Results. We find a conservative value $\Delta V = (1 \pm 5)$ km s^{-1} (1σ C.L.), which when interpreted in terms of $\Delta F/F$ gives $\Delta F/F < 2 \times 10^{-5}$. Independent methods restrict the μ-variations at the level of $\Delta\mu/\mu < 1 \times 10^{-7}$ at $z = 0.7$ (look-back time $t_{z0.7} = 6.4$ Gyr). Assuming that temporal variations in μ, if any, are linear, this leads to an upper limit on $\Delta\mu/\mu < 2 \times 10^{-7}$ at $z = 5.2$ ($t_{z5.2} = 12.9$ Gyr). From both constraints on $\Delta F/F$ and $\Delta\mu/\mu$, one obtains for the relative change in α the estimate $\Delta\alpha/\alpha < 8 \times 10^{-6}$, which is at present the tightest limit on $\Delta\alpha/\alpha$ at early cosmological epochs.

Key words. elementary particles – line: profiles – techniques: radial velocities – galaxies: high-redshift

1. Introduction

Space-time variations in the dimensionless physical constants such as the fine-structure constant, $\alpha = e^2/(\hbar c)$, and the electron-to-proton mass ratio, $\mu = m_{\rm e}/m_{\rm p}$, are predicted within the framework of grand unification theories, multidimensional theories, and scalar field theories (for a review, see Uzan 2011). These constants mediate the strengths of fundamental forces. In essence, α is the coupling constant of the electromagnetic interaction and $m_{\rm e}$ is related to the vacuum expectation value of the Higgs field, i.e., to the scale of the weak nuclear force, whereas $m_{\rm p}$ is proportional to the quantum chromodynamic scale, $\Lambda_{\rm QCD}$. Hence, μ probes the ratio of the weak to strong forces of nature. If detected, a variation in any of these constants would be a manifestation of the need to develop new theories since the standard model of particle physics does not predict any variations in fundamental constants.

Experimentally, the variations in the dimensionless constants can be measured by analyzing the relative positions of atomic and molecular transitions measured in both laboratory and astronomical objects. At present, the most accurate laboratory results on temporal α- and μ-variations are $\dot\alpha/\alpha = (1.6 \pm 2.3) \times 10^{-17}$ yr^{-1} (Rosenband et al. 2008) and $\dot\mu/\mu = (1.6 \pm 1.7) \times 10^{-15}$ yr^{-1} (Blatt et al. 2008). For values of $\alpha(t)$ and $\mu(t)$ that are linearly dependent on cosmic time t, these limits correspond to constraints at redshift $z \sim 2$ (look-back time $t_{z2} \sim 10$ Gyr) of $|\Delta\alpha/\alpha| < 0.4$ ppm (1 ppm $= 10^{-6}$) and $|\Delta\mu/\mu| < 30$ ppm, where $\Delta\alpha/\alpha$ (or $\Delta\mu/\mu$) is a fractional change in α between a reference value α_1 and a value α_2 measured in a cosmic object given by $\Delta\alpha/\alpha = (\alpha_2 - \alpha_1)/\alpha_1$.

The most accurate astronomical measurements of the cosmological μ-variation are performed in the radio range, which constrain $\Delta\mu/\mu$ at the level of 0.3 ppm at $z = 0.89$ (Ellingsen et al. 2012) and 0.1 ppm at $z = 0.69$ (Kanekar 2011). The lowest spectroscopic limits on α are $|\Delta\alpha/\alpha| < 3$ ppm at $z = 0.77$ obtained from radio observations (Kanekar et al. 2012) and the same order of magnitude $|\Delta\alpha/\alpha| \lesssim 3$ ppm at $z \sim 2$–3 derived from optical spectra of quasars (Agafonova et al. 2011; Molaro et al. 2008; Srianand et al. 2007; Quast et al. 2004). To complement these results, the measurements of Murphy et al. (2003) claim detection of an α-variation in about 140 absorption systems from quasar spectra observed with the Keck telescope $\Delta\alpha/\alpha = -5.4 \pm 1.2$ ppm in the range $0.2 < z < 3.7$. However, Griest et al. (2010) showed that the wavelength calibration of these Keck spectra was affected by systematic and unexplained errors of ~500 m s^{-1}, which transformed into an error of $\sigma_{\Delta\alpha/\alpha} \sim 30$ ppm. The Keck result was not confirmed by the analysis of the VLT spectra of quasars acquired from the southern hemisphere by Webb et al. (2011), who found a positive signal of $\Delta\alpha/\alpha = 6.1 \pm 2.0$ ppm at $z \gtrsim 1.8$ in about 150 systems, and proposed a model of a cosmic dipole to reconcile their Keck and VLT findings. A tentative detection of the change in α of $\Delta\alpha/\alpha = -3.1 \pm 1.2$ ppm was also reported by Kanekar et al. (2010) based on observations of OH 18 cm lines at $z = 0.25$.

At earlier cosmological epochs $z > 4$, only a handful of spectral measurements have been able to provide direct constraints

on the temporal variations in α and μ. Some time ago, we suggested a few methods to probe these variations at high redshifts by using far-infrared, sub-mm, and mm transitions in atoms, ions, and molecules usually observed in Galactic and extragalactic sources (Kozlov et al. 2008; Levshakov et al. 2008; Levshakov et al. 2010a). The advantage of fine-structure (FS) transitions is that they have the sensitivity to an α-variation that is about 30 times higher than that of UV transitions employed in optical spectroscopy (Levshakov et al. 2008, hereafter L08): if $\Delta\alpha/\alpha \neq 0$, then the frequency shift $\Delta\omega/\omega_{\rm fs} \equiv (\omega_{z,\rm fs} - \omega_{\rm fs})/\omega_{\rm fs} = 2\Delta\alpha/\alpha$. To take advantage of the high sensitivity of the FS transitions in differential measurements of α, we suggested to take as a reference the low lying rotational lines of carbon monoxide CO since the rotational frequencies of light molecules are independent of α but sensitive to the value of μ, $\Delta\omega/\omega_{\rm rot} = \Delta\mu/\mu$. In case of variations in α and/or μ over cosmic time, one should observe the apparent redshifts of the FS and rotational lines differ of $\Delta z/(1+z) \equiv \Delta V/c = \Delta F/F$, where $F = \alpha^2/\mu$, ΔV is the difference of the apparent radial velocities, and c is the speed of light (L08). The implementation of this method has resulted in $\Delta F/F < 100$ ppm at $z = 6.42$, and $\Delta F/F < 150$ ppm at $z = 4.69$ (L08), and $\Delta F/F < 85$ ppm over the redshift interval $z = 2.3$–4.1 (Curran et al. 2011).

In the present Letter, we show that the [C I]/CO emission discovered by Combes et al. (2012, hereafter CRR) towards the lensed galaxy HLSJ091828.6+514223 at $z = 5.2$ allows us to significantly improve this limit. We note that the look-back time is $t_{z5.2} = 12.9$ Gyr for the cosmological parameters H_0:Ω_b:Ω_c:Ω_Λ = 70.5:0.046:0.228:0.726 (Hinshaw et al. 2009), which is about 94% of the total age of the Universe.

2. Observations and results

Details on observations of the $z = 5.2429$ lensed galaxy HLSJ091828.6+514223 are given in CRR. Here we concentrate on the CO(7–6)/[C I](2–1) data since both lines were observed simultaneously with the same 2mm receiver at the IRAM-interferometer (PdBI). The spectra were reduced with the channel width of $\Delta_{\rm ch} = 46.4$ km s^{-1}, and the resulting noise rms was approximately 0.95 mJy per channel.

The observed spectra of CO($J = 7$–6) and [C I]($J = 2$–1) are shown in Fig. 1. We clearly detect two subcomponents separated by $\simeq$510 km s^{-1} and provide in Table 2 in CRR the parameters for a wider and stronger "red" component of linewidth (FWHM) $w_r \simeq 540$ km s^{-1}, and a narrow and weaker "blue" component of $w_b \simeq 150$ km s^{-1}. We note that the CO(7–6) and [C I](2–1) lines, thanks to their close rest-frame frequencies (806651.806 MHz and 809341.97 MHz, respectively), were observed within one bandwidth, thus their relative positions are free from possible instrumental systematics.

In CRR, the profiles of [C I](2–1) and CO(7–6) were fitted by two simple Gaussians (for the blue and red components) centered at $V_b = -530 \pm 9$ km s^{-1} and 20 ± 14 km s^{-1} for the former line and at $V_r = -510 \pm 30$ km s^{-1} and 4 ± 10 km s^{-1} for the latter (Table 2 in CRR), i.e., the velocity offset between them is $\Delta V \equiv V_{\rm rot} - V_{\rm fs} = 20 \pm 31$ km s^{-1} (blue) and -16 ± 17 km s^{-1} (red). We note that the precision of a single Gaussian line center is $\sigma = 0.69{\rm rms}\sqrt{\Delta_{\rm ch} w}/S_0$ (Landman et al. 1982), where S_0 is the peak intensity and w the linewidth. For the parameters $w \sim 150$ km s^{-1}, $\Delta_{\rm ch} \sim 46$ km s^{-1} rms $\sim$1 mJy, and $S_0 \sim 10$ mJy (cf. Fig. 1), one finds $\sigma \sim 6$ km s^{-1}, which is slightly smaller than the error σ_{V_b} quoted above.

In the present study, we employ a different – model-free – method to measure ΔV. We adopt our approach because despite their complexity, the CO(7–6) and [C I](2–1) lines have almost identical shapes (the scaling factor between their intensities is $\approx$1.6, as indicated in Table 2 in CRR). The procedure ("sliding distance") is realized in the following way: one of the chosen profiles (e.g., T_1 for CO) is fixed and the other (T_2 for [C I]) is shifted relative to T_1 sequentially in small steps, δv, within the velocity interval $[V_1, V_2]$. At each step, a value of Θ^2 – the sum of squares of the intensity differences over n points within the line profile – is to be calculated $\Theta^2(\delta v) = \sum_{j=1}^{n}[T_{1,j} - T_{2,j}(\delta v)]^2$, where Θ is a kind of distance between the curves, and Θ^2 depends parabolically on δv that has its minimum value when the profiles are aligned. The velocity at this minimum is taken as the offset, ΔV, between the two profiles.

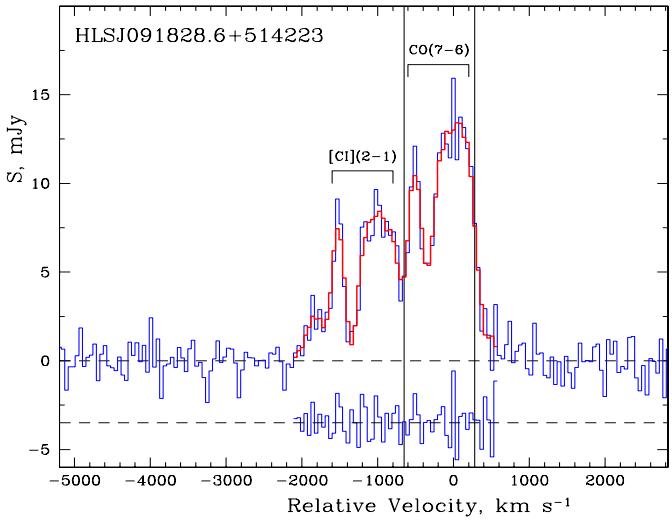

Fig. 1. The CO(7–6) and [C I](2–1) emission lines (blue color histogram) towards the lensed galaxy HLSJ091828.6+514223. The velocity scale is given relative to $z = 5.2429$. The red component of the CO(7–6) line is centered at zero velocity. Its blue component is seen at $V = -510$ km s^{-1}. The red and blue components of [C I](2–1) are shifted with respect to CO(7–6) at -999.8 km s^{-1} owing to their different rest-frame frequencies. Two vertical lines indicate the window used in the bootstrap calculations. The residuals between the original and smoothed data (red color histogram) are shown at the bottom.

In the rest frame, the Doppler velocity shift between the frequencies of [C I](2–1) and CO(7–6) is $\Delta V_0 = -999.8$ km s^{-1}. From Fig. 1, it can be seen that there is a weak component at $V \simeq -1800$ km s^{-1} in the [C I](2–1) profile[1] that may be present in the CO(7–6) profile as well, thus distorting part of the [C I](2–1) profile around $V \simeq -800$ km s^{-1}. To eliminate the influence of this blending on the minimum of Θ^2, the intensity differences were calculated only in the velocity window $-650 < V < 280$ km s^{-1} (marked by the vertical lines in Fig. 1). In addition, to ensure approximately the same intensities in both profiles, the intensity of [C I](2–1) was multiplied by 1.6 (Fig. 2).

The function Θ^2 takes a minimum value at $\Delta V = 0.8$ km s^{-1} (red line in Fig. 3), i.e., the [C I](2–1) line is shifted by -0.8 km s^{-1} relative to CO(7–6). The error in this offset can be estimated by a bootstrap method, where artificial data samples are created based on the statistical properties of the reference data set. In the present context, this means that we have to create spectral profiles that are statistically equivalent to the

[1] This negative velocity wing in [C I](2–1) could be related to the gas outflows (galactic winds) often seen in ultra-luminous infrared galaxies (CRR).

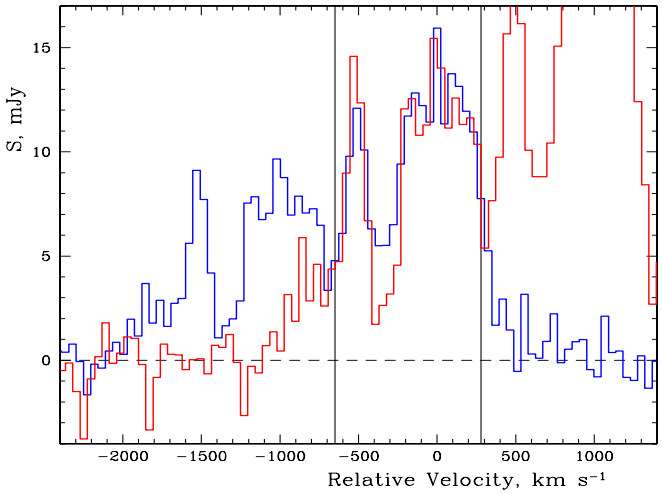

Fig. 2. Same as Fig. 1, but the original spectrum is shifted to +999.8 km s^{-1} (red color histogram) and its intensity is zoomed by a factor 1.6 to be comparable with the CO(7–6) spectrum within the window marked by two vertical lines. This window is used in the bootstrap calculations.

observed ones. In Fig. 1, we find both blue- and redward of the emission profiles the extended parts of the noise spectrum. The statistical analysis of these parts of the spectrum shows that the noise fluctuations are purely Gaussian (i.e., uncorrelated, with zero skewness and excess kurtosis) with a dispersion of 0.95 mJy. In a subsequent step, we obtain an emission-line template, i.e., a noise-free emission-line spectrum. Since the fitting of the Gaussian profiles may be uncertain because of the above-mentioned blending, the template was prepared by filtering the original data. We used a symmetrical Savitzky-Golay filter, which does not introduce any shifts into the filtered data (Savitzky & Golay 1964). The filtered profile is shown by the red color histogram in Fig. 1. The size of the filtering window ($n = 7$) was chosen from the condition that the dispersion in the residuals (differences between observed and filtered data) in the velocity range of the observed emission should be equal to the dispersion in the noise in the emission-free regions (Fig. 1). Artificial emission spectra (1000–10 000 realizations) were generated by adding the noise fluctuations taken from the normal distribution of zero mean and dispersion of 0.95 mJy to the template and the minimization of Θ^2 was performed as described above. Examples of the $\Theta^2(\delta v)$ curves for single realizations are shown in Fig. 3. The resulting distribution of the velocity offsets ΔV between the CO(7–6) and [C I](2–1) profiles is plotted in Fig. 4. It is purely normal with the mean of 0.8 km s^{-1} and dispersion of 4.6 km s^{-1}.

In calculations, different windows (indicated by vertical lines in Fig. 1) were used to estimate the influence of the possible blending in the pair [C I]/CO on the value of the velocity shift. The dispersion of the ΔV distribution was found to be very stable, varying by only a few percent, whereas the mean of the distribution slightly shifted from the above value of 0.8 km s^{-1} when $[V_1, V_2] = [-650, 280]$ km s^{-1} to 0.07 km s^{-1} at $[V_1, V_2] = [-650, 0]$ km s^{-1}. Thus, as a conservative estimate the value of $\Delta V = 1 \pm 5$ km s^{-1} (1σ C.L.) can be taken for the velocity offset between the CO(7–6) and [C I](2–1) lines. If one interprets this offset in terms of $\Delta F/F$, then $\Delta F/F < 17$ ppm. Taking into account that $\Delta\mu/\mu < 0.1$ ppm at $t_{z0.7} = 6.4$ Gyr and that the linearly extrapolated limit at $t_{z5.2} = 12.9$ Gyr, $\Delta\mu/\mu < 0.2$ ppm, is two orders of magnitude lower than the limit on $\Delta F/F$, one finds a constraint on the α-variation at $z = 5.2$ of $\Delta\alpha/\alpha < 8$ ppm.

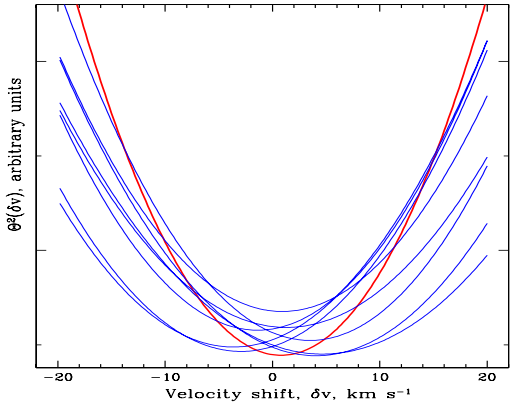

Fig. 3. Examples of the $\Theta^2(\delta v)$ curves for the CO(7–6) and [C I] profiles shown in Fig. 2. The curves were generated by a bootstrap method as described in Sect. 2. The red line shows $\Theta^2(\delta v)$ of the original data set.

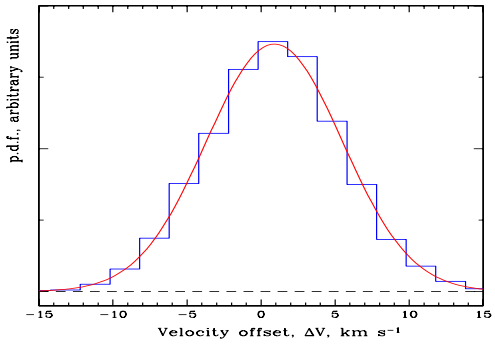

Fig. 4. Bootstrap histogram (probability density function, p.d.f.) of the velocity offset ΔV between the CO(7–6) and [C I](2–1) profiles shown in Fig. 2. Gaussian fit corresponds to $\Delta V = 0.8 \pm 4.6$ km s^{-1} (1σ C.L.).

3. Discussion and conclusions

By minimizing Θ^2, we have estimated the velocity offset ΔV between the CO(7–6) and [C I](2–1) profiles with the precision of 5 km s^{-1}, which has provided an upper limit to the F variability at $z = 5.2$ that is an order of magnitude lower than the limit found in a previous survey of the redshifted pairs of [C I]/CO lines between $z = 2.3$ and 4.1 (Curran et al. 2011). For comparison, in the Milky Way the [C I]/CO pairs restrict $\Delta F/F$ at the level of $|\Delta F/F| < 0.4$ ppm (Levshakov et al. 2010a) leading to a limit on $|\Delta\alpha/\alpha| < 0.2$ ppm since the spatial variations in μ are restricted to $|\Delta\mu/\mu| < 0.03$ ppm in the disk of the Milky Way (Levshakov et al. 2010b; Levshakov et al. 2010c; Levshakov et al. 2011; Ellingsen et al. 2011).

The uncertainty of 5 km s^{-1} is a statistical error determined by the properties of the current observational data, such as the S/N ratio, spectral resolution, and spectral line-intensity gradients. However, there may be systematic errors that contribute to the total error budget. In the present case, two potential sources of systematic errors are apparent: (*i*) velocity shifts caused by observational conditions; and (*ii*) velocity shifts due to non-co-spatial distributions of the compared species. The first source is eliminated thanks to the unique characteristics of the emission pair [C I]/CO of the $z = 5.2$ galaxy – narrow linewidths of the subcomponents and close rest frame-frequencies – which allow us to observe them with the same receiver and within the same frequency band. In this way, we can avoid systematic uncertainties in the velocity scale calibration during long exposure times.

We consider possible kinematic segregation between CO and C^0. In the Milky Way and in nearby galaxies, the C^0 emission is closely associated with that of CO (for references, see Levshakov et al. 2010a; Curran et al. 2011). The carbon-bearing species C^0, C^+, and CO are observed in photodissociation regions (PDRs) – neutral regions where chemistry and heating are regulated by the far-UV photons (Hollenbach & Tielens 1999). Photons of energy higher than 11.1 eV dissociate CO into atomic carbon and oxygen. Since the C^0 ionization potential of 11.3 eV is quite close to the CO dissociation energy, neutral carbon can be quickly ionized. This suggests that there is a chemical stratification of the PDR between the lines $C^+/C^0/CO$ with increasing depth from the surface of the PDR. The observed correlation between the spatial distributions of C^0 and CO can be explained by clumpy PDR models (e.g., Meixner & Tielens 1995; Spaans & van Dishoeck 1997; Papadopoulos et al. 2004). In the observed $z = 5.2$ galaxy, the derived excitation temperature of the higher-J CO lines, $T_{\rm ex} = 40$ K, and the gas density $n_{\rm H_2} = 3.5 \times 10^3$ cm^{-3} (CRR) just corresponds to the critical density of $n_{\rm cr} \approx 3 \times 10^3$ cm^{-3} required to excite collisionally the $J = 2$ level of the ground state triplet of C^0 (e.g., Levshakov et al. 2010a). Thus, we can assume that in the present case the distributions of CO and C^0 closely trace each other. At $z = 5.2$, we also observe integrated emission over all molecular gas-clouds within the galaxy. This naturally leads to an averaging of the random fluctuations of the line-of-sight velocity components $V_{\rm CO}$ and $V_{\rm [CI]}$ and a suppression of the input produced by possible deviations from the co-spatial distribution of the compared species and the velocity shift between them.

The uncertainties in the rest-frame frequencies of the analyzed transitions can be neglected since they are much smaller than the error in the velocity offset, $\sigma_{\Delta V} = 5$ km s^{-1} (Klein et al. 1998; Müller et al. 2005).

Thus, we conclude that the limit obtained on the variability of $\Delta F/F$ at $z = 5.2$ is robust and free from significant systematic errors. The error of 5 km s^{-1} in the velocity offset between CO(7–6) and [C I](2–1) is dominated by the noise fluctuations and can be reduced if observations of higher S/N are performed. However, even the present constraint on $\Delta\alpha/\alpha \equiv \Delta V/2c = 2 \pm 8$ ppm casts doubts on the dipole model of Webb et al. (2011), which predicts $\Delta\alpha/\alpha = -12 \pm 3$ ppm for the galaxy HLSJ091828.6+514223.

Acknowledgements. S.A.L., I.I.A., and M.G.K. are supported by DFG Sonderforschungsbereich SFB 676 Teilprojekt C4, and by the RFBR grant 11-02-12284-ofi-m-2011.

References

Agafonova, I. I., Molaro, P., Levshakov, S. A., & Hou, J. L. 2011, A&A, 529, A28
Blatt, S., Ludlow, A. D., Campbell, G. K., et al. 2008, Phys. Rev. Lett., 100, 140801
Combes, F., Rex, M., Rawle, T. D., et al. 2012, A&A, 538, L4 [CRR]
Curran, S. J., Tanna, A., Koch, F. E., et al. 2011, A&A, 533, A55
Ellingsen, S., Voronkov, M., & Breen, S. 2011, Phys. Rev. Lett., 107, 270801
Ellingsen, S., Voronkov, M., Breen, S., & Lovell, J. E. J. 2012, ApJ, 747, L7
Griest, K., Whitmore, J. B., Wolfe, A. M., et al. 2010, ApJ, 708, 158
Hinshaw, G., Weiland, J. L., Hill, R. S., et al. 2009, ApJS, 180, 225
Hollenbach, D. J., & Tielens, A. G. G. 1999, Rev. Mod. Phys., 71, 173
Kanekar, N. 2011, ApJ, 728, L12
Kanekar, N., Chengalur, J. N., & Ghosh, T. 2010, ApJ, 716, L23
Kanekar, N., Langston, G. I., Stocke, J. T., Carilli, C. L., & Menten, K. L. 2012, ApJ, 746, L16
Klein, H., Lewen, F., Schieder, R., et al. G. 1998, ApJ, 494, L125
Kozlov, M. G., Porsev, S. G., Levshakov, S. A., et al. 2008, Phys. Rev. A, 77, 032119
Landman, D. A., Roussel-Dupre, R., & Tanigawa, G. 1982, ApJ, 261, 732
Levshakov, S. A., Reimers, D., Kozlov, M. G., et al. 2008, A&A, 479, 719 [L08]
Levshakov, S. A., Molaro, P., & Reimers, D. 2010a, A&A, 516, A113
Levshakov, S. A., Molaro, P., Lapinov, A. V., et al. 2010b, A&A, 512, A44
Levshakov, S. A., Lapinov, A. V., Henkel, C., et al. 2010c, A&A, 524, A32
Levshakov, S. A., Kozlov, M. G., & Reimers, D. 2011, ApJ, 738, 26
Meixner, M., & Tielens, A. G. G. M. 1995, ApJ, 446, 907
Molaro, P., Reimers, D., Agafonova, I. I., & Levshakov, S. A. 2008, EPJST, 163, 173
Müller, H. S. P., Schlöder, F., Stutzki, J., & Winnewisser, G. 2005, J. Mol. Struct., 742, 215
Murphy, M. T., Webb, J. K., & Flambaum, V. V. 2003, MNRAS, 345, 609
Papadopoulos, P. P., Thi, W.-F., & Viti, S. 2004, MNRAS, 351, 147
Quast, R., Reimers, D., & Levshakov, S. A. 2004, A&A, 415, L7
Rosenband, T., Hume, D. B., Schmidt, P. O., et al. 2008, Science, 319, 1808
Savitzky, A., & Golay, M. J. E. 1964, Anal. Chem., 36, 1627
Spaans, M., & van Dishoeck, E. F. 1997, A&A, 323, 953
Srianand, R., Chand, H., Petitjean, P., & Aracil, B. 2007, Phys. Rev. Lett., 99, 239002
Uzan, J.-P. 2011, LRR, 14, 2
Webb, J. K., King, J. A., Murphy, M. T., et al. 2011, Phys. Rev. Lett., 107, 191101